Fermilab

TM-929
1751.000

THE ABORT DUMP FOR THE ENERGY SAVER/DOUBLER AND MAIN RING

T. E. Toohig

December 6, 1979

I. Introduction

The re-allocation of the straight sections of the accelerator for Doubler/Collider operation requires the removal of the Main Ring abort to CO from its present location at DO. The Doubler abort will be installed at the same location. The present abort at DO disposes of the beam by aborting it over several turns against an aluminum block which is the limiting aperture for the Main Ring orbit. The resulting spray of radiation is absorbed further downstream in the machine, principally by two dipole carcasses. The residual activity is in the 500 mrem/hr range which makes maintenance very difficult. The sensitivity of the Doubler magnets to quenching by radiation makes it desirable to avoid this spray by extracting the aborted beam in a single turn and disposing of it outside the ring.

To cope with both the quench problem and the problem of residual activation, there must be enough room between the dump and the accelerator orbits to install shielding sufficient to reduce to tolerable levels both the dynamic radiation from the dump and the residual activation in the vicinity of the magnets.

II. General Considerations

A nearly-final version of the abort system for the Doubler as described in the "Blue Book" is reproduced in Figure 1. At 1 TeV the

aborted beam is very stiff so the separation between the machine orbit and the abort is due primarily to the curvature of the accelerator orbit. The rate of orbit separation from C12 to C13, which is relevant for the the abort, is approximately 6" per 10'.

The integrity of Main Ring tunnel structure requires symmetrical loading on the precast "hoops". To maintain this loading the tunnel must be fully excavated on both sides for the full length of any excavation required to install the abort system. The differential excavation cost for moving the dump downstream to gain transverse shielding is approximately $1K/in. transverse. The incremental cost of the additional shielding is approximately $5K/in. transverse in increasing the width by 2'. The addition of steel beyond the design 2' surrounding the core exceeds the yield point of the soil, requiring caissons or pilings to support the load. The pilings which are the cheaper solution, add an additional $4K/in. for a 2' increment. Finally, if the dump is not in or contiguous to the tunnel for direct inspection, a one-time cost for elaborate monitoring sumps and an annual estimated $6K/yr for monitoring must be added to the cost. As the dump moved further out from the ring, a dump "beam" may be required to keep surface levels well below public access levels. For these reasons provision of extra shielding for "insurance" can only be done at a high cost in initial construction and subsequent operation, of the order of $10K/in. for significant increments.

The dump shown in Figures 2 and 3 has been evolved in the light of these considerations. Six constraints enter into the design; it must be capable of withstanding the instantaneous heating caused by absorbing

the full intensity of the beam in 20 μsec; it must provide sufficient absorption and scattering for muons in the forward direction to ensure that no significant flux of muons reaches an exposed position outside the site boundary; the inclusion of uranium to provide this absorption adds a requirement for absorber prior to the uranium to preclude production of fissile materials; transversely, the shield must reduce the dynamic and residual radiation levels in the Main Ring tunnel, as noted above, to protect the superconducting magnets and personnel working on them, and to protect the ground water environment.

The adequacy of the dump may be evaluated by comparison with experimental data and by computer modeling using such codes as the Fermilab CASIM, or the CERN programs MAGKA and CYLKAZ.

III. Analysis

1. Thermal Shock

The use of a segmented BeO core as the first element in the dump is modeled on the experience of the Neutrino Department with BeO targets for neutrino production. In Appendix I an evaluation of the abort core is made on the basis of neutrino experience. This evaluation indicates that the abort dump as designed is adequate to withstand the thermal shock caused by single-turn extraction of 2×10^{13} ppp from the Tevatron.

2. Dynamic and Residual Radiation in the Main Ring Tunnel

The transverse shielding provided by the dump as sketched in Figure 2, consists of 3" of BeO, 9" of Al, 2' of Fe, and 10" of concrete from the beam axis to the inside wall of the Main Ring tunnel. This shielding must be evaluated in terms of both the instantaneous radiation

striking the superconducting magnets when 2×10^{13} 1 TeV protons are absorbed in 20 μsec, and of the residual radiation resulting from dumping 3.5×10^{17} protons/yr. As noted above, this evaluation can be done by comparison with experiment and by computational techniques.

a. Experimental Comparison

In Appendix IIa the dynamic levels are estimated by scaling from measurements made during operation of the beam dump experiment E439 in the Meson Area. The residual levels are scaled from measurements made during dismantling of that beam dump. The configuration of the core of the E439 dump illustrated in Appendix IIa is very closely a duplicate of the proposed abort dump. The integrated proton flux for E439 during a 6-month period was $> 2.5 \times 10^{16}$ protons, so no great extrapolation of data is required. From these data, as detailed in Appendix IIa, the residual levels in the abort dump at the outer surface of the steel would be $\sim$ 40 mrad/hr and the residual dose levels inside the tunnel would be < 10 mrem/hr at the wall. The dynamic level for 2×10^{13} protons aborted in a single pulse will be $\sim$ 400 R/pulse.

b. Calculations

A calculation of the same quantities by Radiation Physics[1] gives at the surface of the steel, 2.28 rad/hr for infinite irradiation with no cooldown and 0.63 rad/hr for an irradiation of 30 days with 1 hour cooldown. This is one to two orders of magnitude above the scaled E439 measurement.*

---

*NAP: A memo from S. Velen to RSO's dated 16 Nov. 1979 states that CASIM overestimates radiation levels by one to two orders of magnitude. This may account for the discrepancy.

The calculations of Van Ginneken for the same geometry but including 10" of concrete for the tunnel wall predict 56 mrad/hr for infinite irradiation and no cooldown. This does not seem to be inconsistent with the E439 measurement allowing for the fact that the E439 measurement involved a limited irradiation time and several days of cooldown. These results are listed in Appendix IIb.

An old calculation by T. White (circa 1968) also reproduced in Appendix IIc would predict $\sim$ 80 mrad/hr at the surface of the steel (165 mrem/hr) for 400 GeV, or $\sim$ 150 mrad/hr at 1 TeV assuming α $E^{0.7}$.

3. Energy Deposition in Doubler Magnets

Irradiation of Doubler magnets can lead to problems of quenching if the instantaneous rates are sufficiently high and of long-term degradation of the superconductor and other magnet components for all levels of irradiation. The problem of long-term deterioration scales directly from the residual radiation calculations above. The problem of quenching the magnets is not a function of the long term average radiation levels, but of the intensity of the individual pulses, nominally 2 x 10^{13} ppp.

a. Experimental Determination

The energy deposition at the inside of the tunnel wall for 2 x 10^{13} ppp is estimated in Appendix IIa from the E439 data. Scaling to 1 TeV and 2 x 10^{13} ppp yields

$$D = 0.8 \text{ mJ/gm}$$

b. Calculations

Van Ginneken has calculated the upper limit for the energy deposition at the inside of the tunnel wall as

$$D \leq 3 \times 10^{-7} \text{ GeV/cm}^3\text{-proton}$$

$$D = 0.1 \text{ mJ/pulse for } 2 \times 10^{13} \text{ ppp}$$

This is about an order of magnitude below the quench level.

4. Ground Water Activation

The modification of the abort dump design to make it contiguous with the Main Ring tunnel eliminates the possibility of the immersion of the dump in ground water with subsequent direct irradiation of the water. There still remains the question of protecting the ground water environment outside the dump.

In Appendix III it is shown that even on extremely conservative assumptions the ground water activity associated with the dump design in Figure 2 is orders of magnitude below the current EPA guidelines.

5. Production of Fissile Materials

The tangent to the Main Ring from the CO straight section entails the shortest distance to the site boundary of any of the six straight sections of the accelerator. The distance to the site boundary at Butterfield Road is 1.7 km, which is less than the range of 1 TeV muons. As outlined in Appendix IVa, it is advantageous to use a depleted uranium core behind the abort dump to absorb and scatter the high energy muons emerging from the back of the dump. However, this raises the spectre of the possibility of production of fissile materials in the U^{238} by absorption of neutrons produced in the hadron cascade. In Appendix Va an estimate is made of the production of Pu^{239} based on

calorimetric studies of the hadronic cascade, assuming that neutrons produced upstream of the uranium are absorbed sufficiently so that their contribution to excitation is negligible relative to the tail of the proton distribution. Under this assumption a fraction of a microgram of Pu^{239} - less than that produced naturally in U^{238} - might be produced in the two tons of U^{238} comprising the core. (The natural occurrence of Pu^{239} in pitchblende ore is 7 parts per million according to the Handbook of Nuclear Energy.)

Van Ginneken has carried out a detailed calculation including 1.5' of concrete between the iron and the uranium. This is shown in Appendix IVd. He finds a production rate of 545 Pu^{239}/incident proton or

$$R_{Pu} \sim 0.07 \text{ gm/yr}$$

assuming 3.5×10^{17} protons/yr. This rate may be further reduced by a factor of 1.5 per 1 foot of concrete.

Cossairt asserts without documentation that under the same conditions

$$R = 1.0 \text{ gm/yr}$$

IV. Conclusions

The Doubler abort dump as sketched in Figures 1 and 2 adequately meets the design constraints relative to environmental and personnel radiation levels. A dose rate for the problem of quenching superconducting magnets is arrived at which must be related to the quench

properties of the magnets. These values must also be understood in terms of long term deterioration of the superconductor and other magnet components.

Discrepancies of several orders of magnitude between the Van Ginneken calculations, and the Radiation Physics calculations need to be understood. The Van Ginneken calculations seem to be consistent with experimental values.

V. References

1. TM-902, D. Cossairt, "Radiation Safety Implications of the Proposed Main Ring/Energy Doubler Abort".

HORIZONTAL BEAM DISPLACEMENT

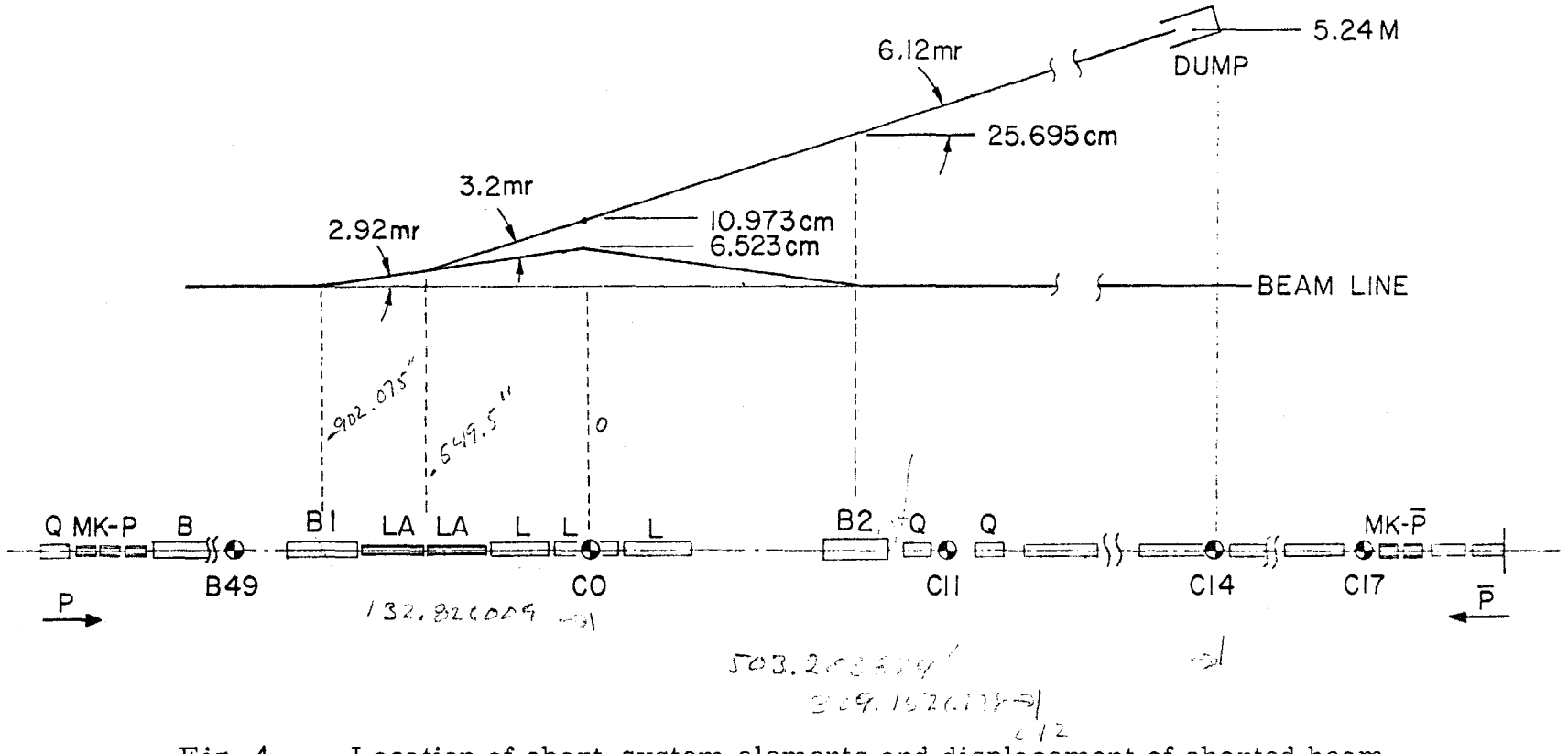

Fig. 1 Location of abort-system elements and displacement of aborted beam.

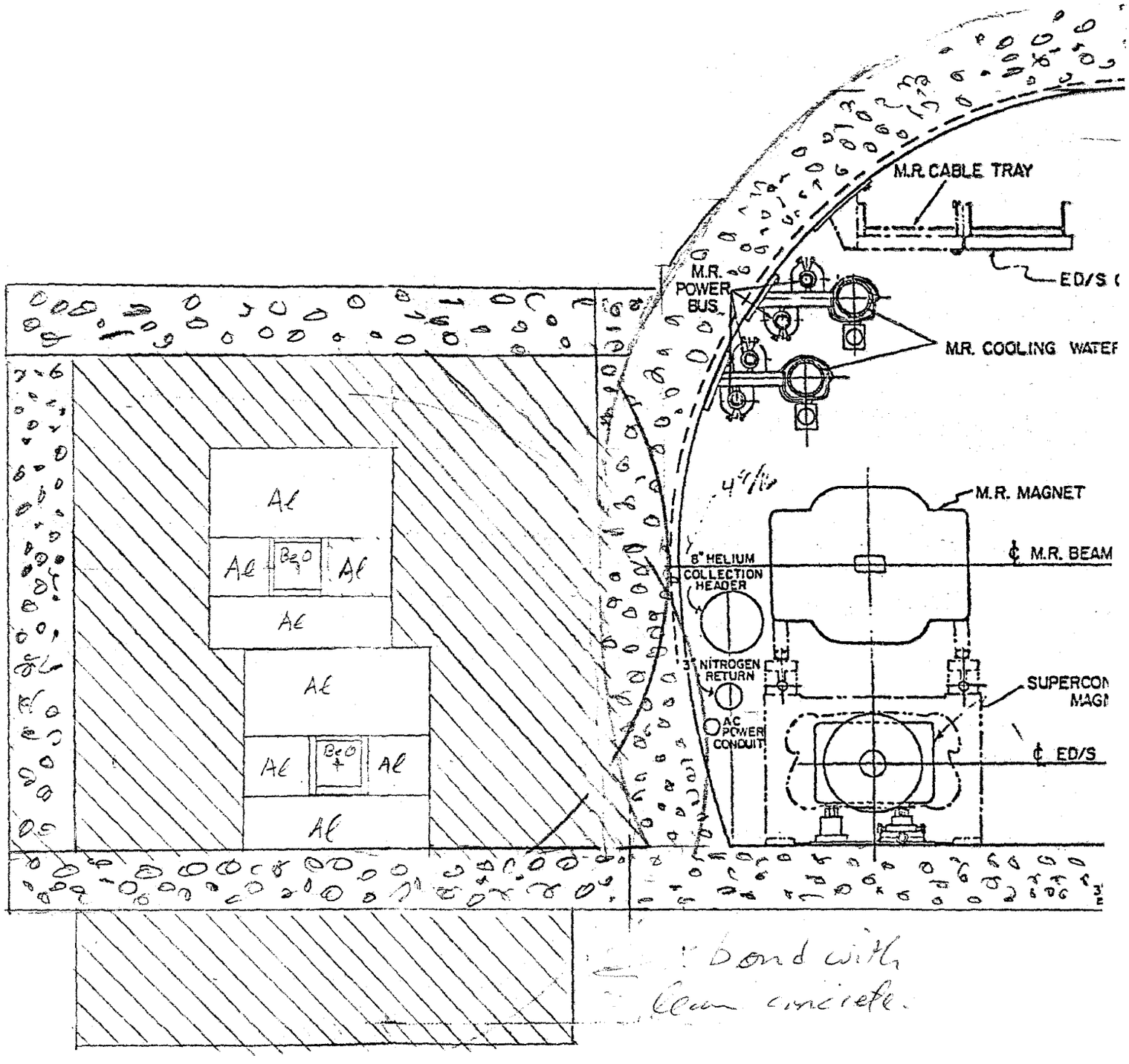

Cross-section at C12 + 50'

1'

Figure 2

NATIONAL ACCELERATOR LABORATORY ENGINEERING NOTE	SECTION	PROJECT	SERIAL-CATEGORY	PAGE
	ED	Abort		6

SUBJECT	NAME	
Abort assembly	T. E. Toohig	
	DATE 8-22-79	REVISION DATE 10-19-79

TM-929

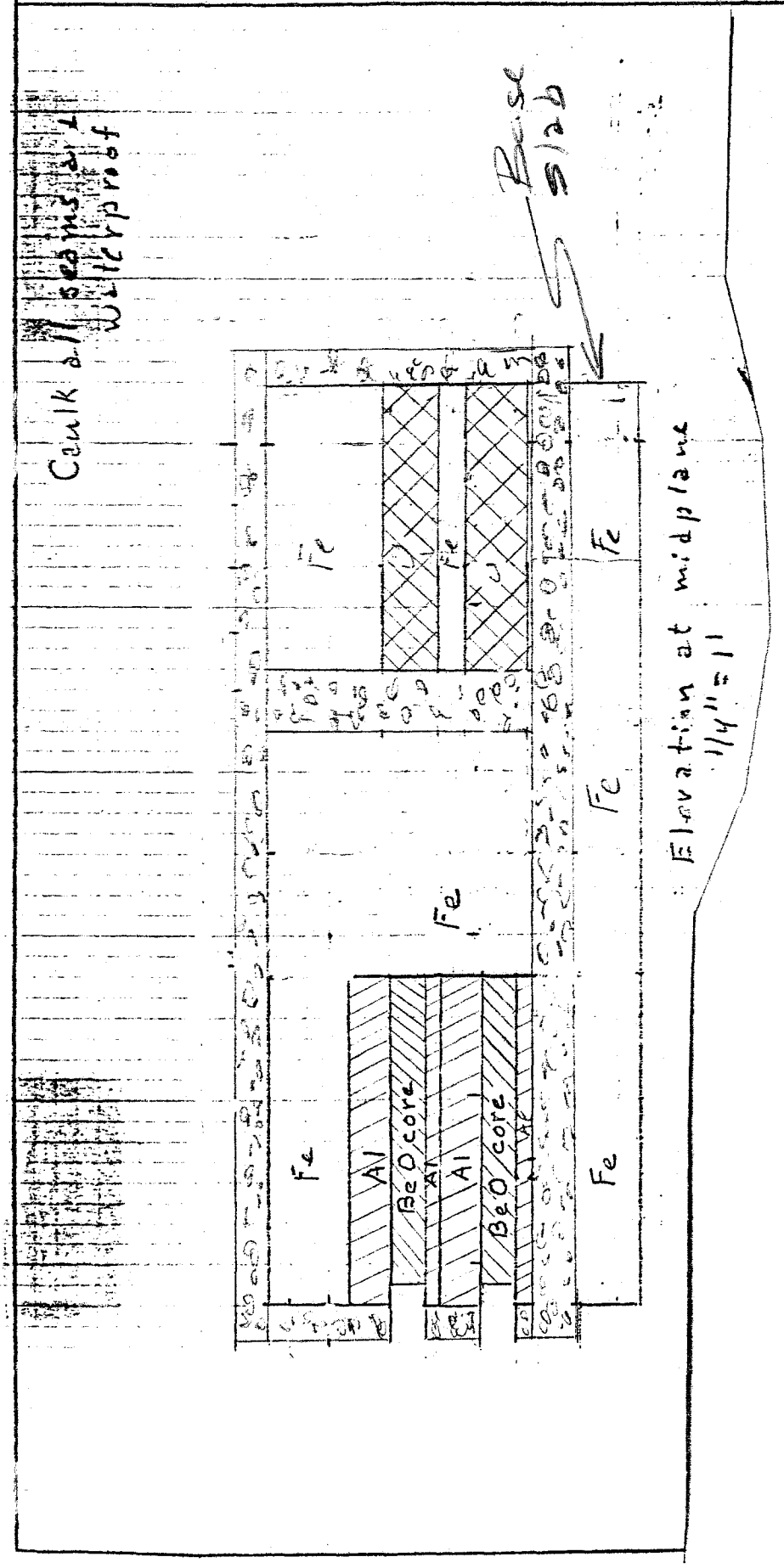

Figure 3

Appendix I

TM-929

Fermilab

September 21, 1979

MEMO TO: File

FROM: T. E. Toohig

SUBJECT: INTEGRITY OF THE BeO TEVATRON ABORT DUMP UNDER FAST SPILL

The experience of the Neutrino Department with a BeO target[1] provides a normalization for the design of the Tevatron abort dump. Cossairt[2] has calculated the relative energy density for one interaction length of BeO as compared with the peak of the cascade as

$$\frac{I(\lambda)}{I(\text{peak})} = \frac{0.024\ \text{GeV/cm}^3/\text{p}}{0.17\ \text{GeV/cm}^3/\text{p}} = \frac{1}{7.1}$$

The Neutrino target has been subjected to a bombardment of 1.2×10^{19} protons in fast spill with a spot size of 1 mm^2 without any degradation as determined by disassembly and inspection.[3]

The beam area of the aborted Tevatron beam at the dump, relative to the Neutrino beam is

$$\frac{A_{\text{TeV}}}{A_{21}} = \frac{\pm 3.3 \times \pm 2.1\ \text{mm}^2}{1\ \text{mm}^2} \simeq 27.7$$

The peak energy density in the dump relative to the Neutrino target is

$$\frac{I_{\text{peak}}}{I_{\nu}} = 7.1 \times \frac{1}{27.7} \times \frac{1000\ \text{GeV}}{400\ \text{GeV}} = 0.6$$

Additionally the maximum dynamic stress is a function of target segmentation length.[4] This further reduces the thermal shock in the abort dump by

$$\frac{\ell_{\text{abort}}}{\ell_{\nu}} = \frac{1\ \text{inch}}{1.5\ \text{inch}} = 0.67$$

The abort thermal shock relative to the (known non-destructive) Neutrino target thermal shock is then

$$\boxed{R = 0.4}$$

1. J. Grimson, "Target for Neutrino Beams", TM-825, Oct. 1979.

2. J. Cossairt, Private Communication. The beam spot size was assumed 1" x 1" uniformly illuminated. This should not be of consequence for the relative energy deposition used here.

3. J. Grimson, Private Communication. The spill length for this particular target was 1 msec. Previous targets of the same design have been subjected to 38 μsec spill without damage.

4. W. Kalbraier, W. C. Middelkoop, P. Sievers, "External Targets at the SPS", CERN Lab II/BT/74-1, Feb. 1974.

TET:eg

cc:
J. R. Orr
H. Edwards
H. Casebolt
F. Turkot
L. Coulson
D. Cossairt

APPENDIX IIa

Scaling of Dose Rate and Residual Activity from E439 Dump Experience

During 1977-1978 Dimuon experiment E439 operated with 400 GeV protons incident on a simple dump at intensities up to 7×10^{11} protons per pulse. The dump configuration as shown in Figure II-1 is similar to the proposed abort dump configuration shown in Figure 2. A total of $\geq 2.5 \times 10^{16}$ protons was targetted over a period of $\sim$ 6 months.

1. Dynamic Levels

The measured level outside the E439 shield was 0.8 mrem/hr for 6×10^{10} ppp and a 10 sec. repetition rate. This scales to 0.0133 mrem/pulse, or

$$\frac{2 \times 10^{13}\text{ppp}}{6 \times 10^{10}\text{ppp}} \times \left(\frac{1000\text{ GeV}}{400\text{ GeV}}\right)^{0.7} \times 0.0133\text{ mrem} = 1.48\text{ mrem/pulse}$$

for 1 TeV, 2×10^{13} ppp.

Scaling back to the outside of the first H block, which approximates the inside of the tunnel wall

$$\dot{D}_{outside} = \dot{D}_H e^{-\Delta\tau/\lambda}$$

$$\dot{D}_H = 1.48\text{ mrem } e^{\frac{1246\text{ gm/cm}^2}{100\text{ gm/cm}^2}}$$

$$= 382\text{ R/pulse}$$

$$D_H \simeq 76\text{ rad/pulse assuming QF} = 5$$

$$\simeq 7600\text{ erg/gm}$$

$$\boxed{D_H \simeq .8\text{ mJ/gm}}$$

2. Residual Levels

The measured residual level at the upstream face of Magnet I immediately behind the target was

$$\dot{D}_I = 800 \text{ mrem/hr}$$

Using Cossairt's calculated fall off for 2' of steel

$$\dot{D}_I = 10.4 \text{ mrem/hr}$$

at the outside of the steel.

On the assumption of 2.5×10^{16} protons targetted in 6 months the average rate is

$$\phi_{439} = 1.6 \times 10^{9} \text{ p/sec}$$

compared with

$$\phi_{abort} = 1.1 \times 10^{10} \text{ p/sec}$$

If we scale this value for 1000 GeV and 3.5×10^{17}/yr, the residual activity at the outside of the steel of the dump is

$$\dot{D}_{res} = \dot{D}_o \times \frac{1.1 \times 10^{10}}{1.6 \times 10^{9}} \times \left(\frac{E_{1000}}{E_{400}}\right)^{0.7}.$$

$$\boxed{\dot{D}_{res} = 37.7 \text{ mrem/hr}} \quad \text{from Fe}$$

The levels inside the tunnel are further substantially decreased by the additional shielding due to the 10" of concrete comprising the wall and the low residual activity of the low-sodium concrete relative to the steel. As measured, the A block alongside the magnet block showed less than 1 mrem/hr of residual on the side nearest the target and no measurable activity on the outside.

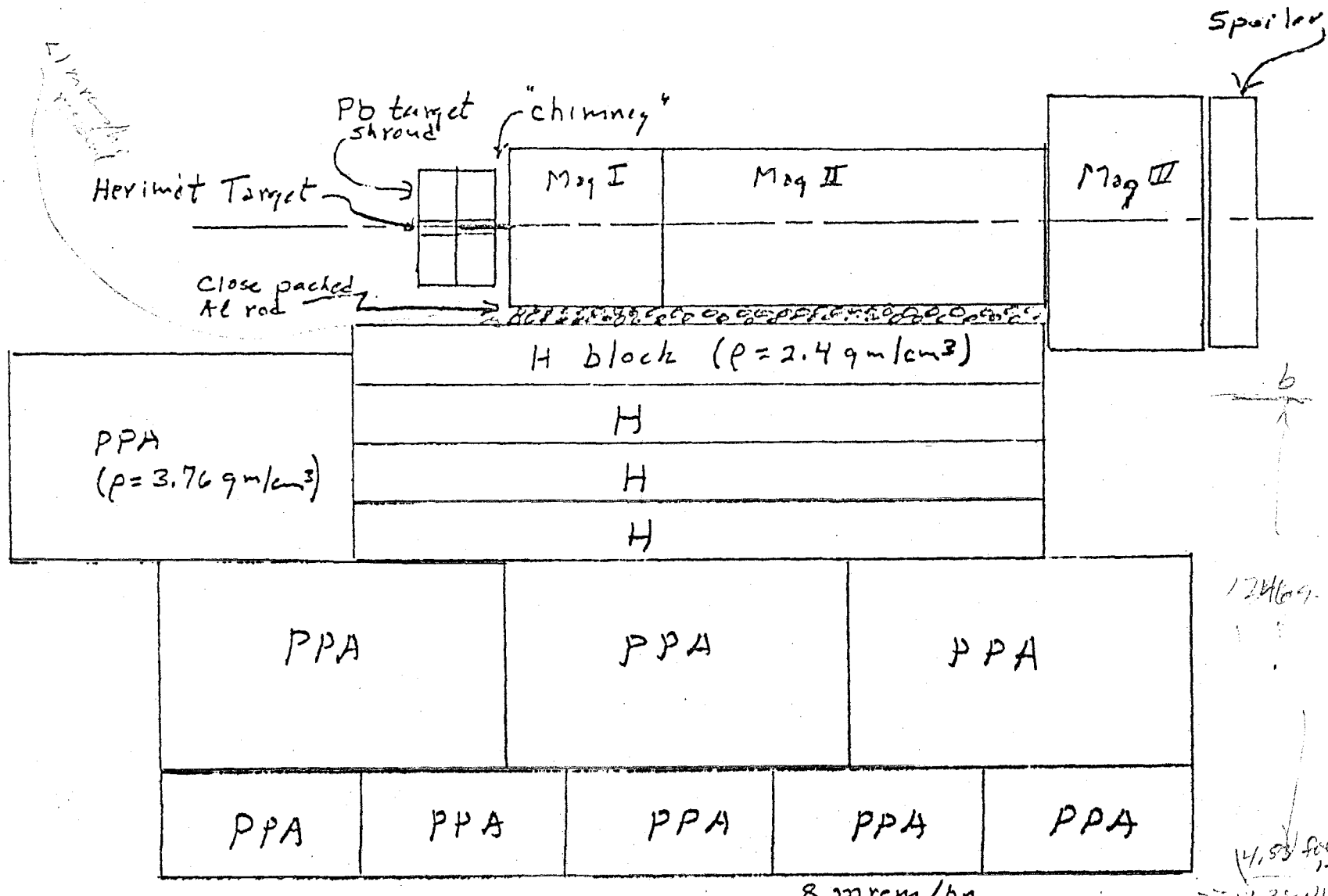

Figure 1

E439 Side Shield Configuration

NAME J. Toohig

DATE 4/21/78

REVISION DATE

Fermilab

Appendix Ib

Fermi National Accelerator Laboratory
P.O. Box 500 • Batavia, Illinois • 60510

November 8, 1979

TO: Tim Toohig

FROM: Don Cossairt Don Cossairt

SUBJECT: Residual Dose Rate and Energy Deposition near the Proposed Revised (11/5/79) Location of the Main Ring Abort.

This is in reply to your recent query concerning residual dose rates and instantaneous radiation levels near the main ring abort. To estimate this I ran CASIM at 1000 GeV for 3" BeO surronded by 1" AL (laterally) surrounded by Fe and estimated the quantities of interest at both 2' and 4' total radial shielding.

The residual activity was calculated following P.J. Gollon in TM 609 (1976) where the dose rate $\dot{D}$ is related to the star production (cm^3. sec) at the surface of the shield by the following:

$$\dot{D} = S\ W$$

where W $(\infty, 0) = 9 \times 10^{-6}$ rad hr^{-1}/ (star.cm^{-3} sec^{-1}) for infinite irradiation with zero cooling time and w (30, 1) = 2.5×10^{-6} rad hr^{-1}/ (star cm^{-3} sec^{-1}) for a 30 day irradiation with 1 day cooldown. These two values of W then bracket reasonable operating conditions.

Using your estimate of 3.5×10^{17} protons/yr (averages to 1.1×10^{10} proton/sec) we have:

A. 2' Radial shield - 2.3×10^{-5} stars/cm^3. proton
   $\dot{D}$ $(\infty, 0) = 2.3 \times 10^{-5}$ stars/ (cm^3. proton) x 1.1×10^{10} proton/sec x W $(\infty,0)$
   = 2.28 rad/hr
   $\dot{D}$ (30,1) = 0.63 rad/hr

B. 4' Radial Shield -3×10^{-7} star/cm^3. proton
   $\dot{D}$ $(\infty, 0)$ = 30 mrad/hr
   $\dot{D}$ (30,1) = 8 mrad/hr

So that an appreciable reduction is achieved by the extra 2 feet. The above numbers are for contact with the Fe shield, geometry will of course reduce these values somewhat in accessable areas.

The energy deposition was read directly from the CASIM output. The conversion is, of course, for iron:

$$1 \frac{\text{GeV}}{\text{cm}^3} = 1 \frac{\text{GeV}}{\text{cm}^3} \times \frac{1 \text{ cm}^3}{7.9 \text{ gm}} \times \frac{1.6 \times 10^{-10} \text{ J}}{\text{GeV}} \times \frac{10^7 \text{ ergs}}{\text{J}} = 2.02 \times 10^{-4} \frac{\text{ergs}}{\text{gm}}$$

thus

$$1 \frac{\text{GeV}}{\text{cm}^3} = 2.02 \times 10^{-6} \text{ rads}$$

A. 2' Radial Shield for 2.5×10^{13} protons during a 20 μsec spill (instantaneous energy deposition).

The maximum energy deposition density is:

$1.5 \times 10^{-6} \frac{\text{GeV}}{\text{cm}^3} \text{ proton}^{-1} \Rightarrow 1.875 \times 10^{12} \frac{\text{GeV}}{\text{cm}^3} \text{ sec}$

$= 3.8 \times 10^8$ ergs/(gm . sec)

B. 4' Radial Shield for same conditions.

7.5×10^{-9} GeV/(cm^3. proton) => 3.1×10^9 GeV/cm^3

$= 6.31 \times 10^5$ ergs/(gram . sec)

If continuous dumping is done at 10 sec cycle time at such intensities

at 2' radial shield we have:

3.8×10^6 rads/sec x 20 μsec = 76 rad/cycle ∿ 27000 rads/hr

at 2' radial shield we have:

6.3×10^3 rads/sec x 20 μsec = 0.1 25 rad/cycle or 45 rad/hr

These too are at the surface of the shielding but would not be expected to fall off by more than a factor of 10 at the location of the superconducting magnets. None of the above depends upon whether uranium is included in the downstream half of the dump.

DC/cm

cc: F. Turkot
H. Edwards
K. Cahill
H. Casebolt
S. Baker
L. Coulson
A. L. Read
File

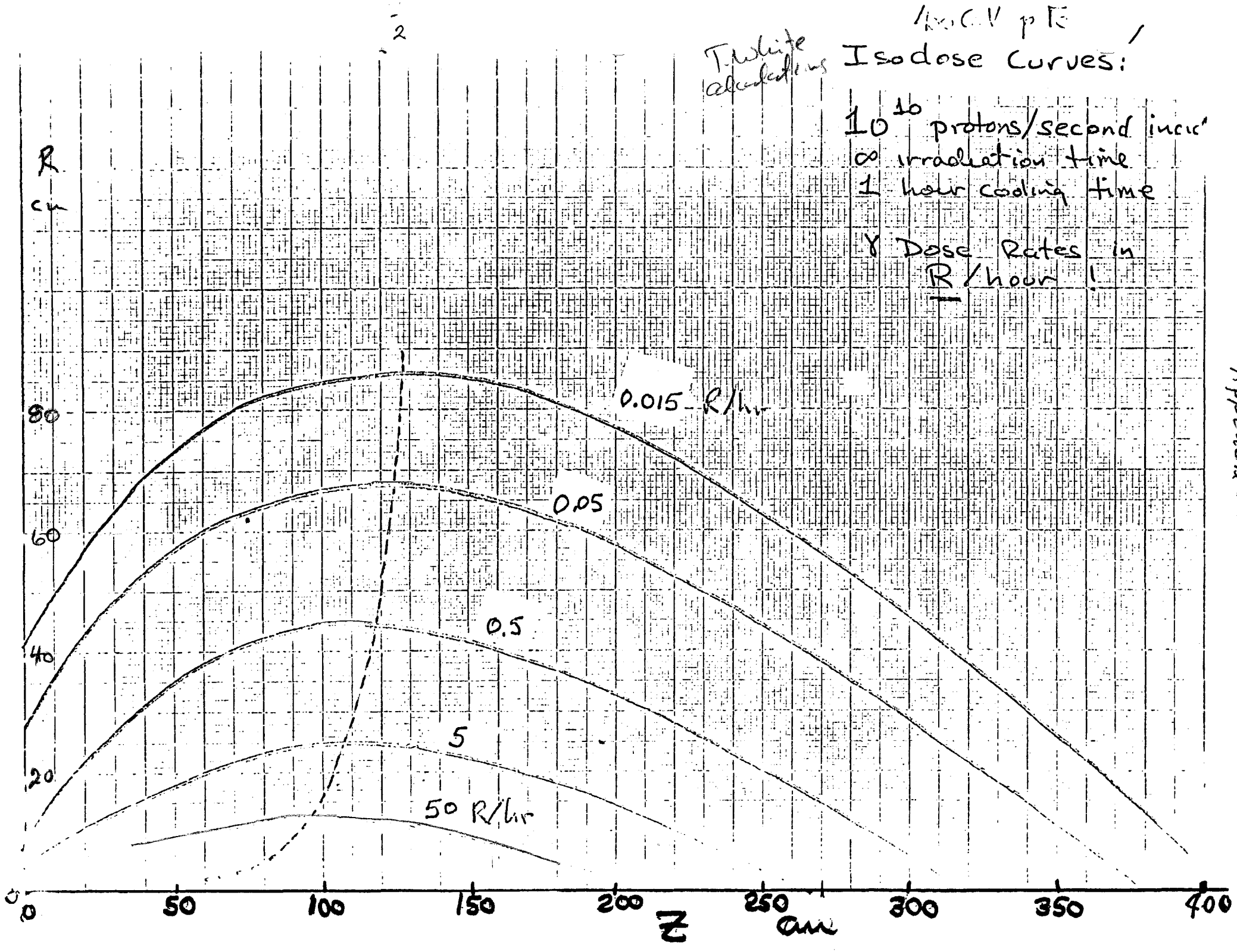
T. White calculations
Isodose Curves:
10^{10} protons/second incid
∞ irradiation time
1 hour cooling time
γ Dose Rates in R/hour !
R cm
0.015 R/hr
0.05
0.5
5
50 R/hr
80
60
40
20
0
50
100
150
200
250
300
350
400
Z cm

APPENDIX III

GROUND WATER ACTIVATION IN THE VICINITY OF THE TEVATRON ABORT DUMP

The proposed design for the Tevatron abort dump is shown in Figure 1. The integrated intensity specification for the dump is 3.5×10^{17} protons per year at 1 TeV. Alan Jonckheere has recently calculated the same problem for the Meson Area high intensity beam dump taking into account the latest EPA and Laboratory restrictions.[1] For simplicity we will scale from his calculation although there are extensive data which indicate that the assumptions underlying his calculations are very restrictive, overestimating the measured losses by several orders of magnitude.[2]

Bearing in mind this caveat, we scale the calculation to the proposed Tevatron abort dump as shown in Figure 2. We assume underdrains around the support slab. Under these circumstances Table I of reference 1 becomes:

Material	Side Shield (cm)	Undershield (cm)	Interaction Length (cm)*
BeO	7.5	7.5	26
Al	22.5	20	35
Fe	60	60	17.3
Concrete	30	30	44.6
Sand & Gravel	60	0	53.6

Table I

*CERN Lab II/BT/74-1, External Targets at the SPS, W. Kalbreier, W. C. Middelkoop, P. Sievers.

Scaling as in reference 1:

$$S \sim \frac{1}{r} \exp\left(-\Sigma X_i/\lambda_i\right)$$

$$S_{side} \sim \frac{1}{180} \exp -\left(\frac{7.5}{26} + \frac{22.5}{35} + 60/17.3 + 30/44.6 + 60/53.6\right)$$

$$\sim 1.14 \times 10^5$$

$$S_{bottom} \sim \frac{1}{118} \exp\ 26 + \frac{20}{35} + \frac{60}{17.3} + \frac{30}{44.6})$$

$$\sim 5.7 \times 10^5$$

$S_{study} = 8 \times 10^{-5}$ (assuming Cossairt is right, but see Velen's memo)

$(S_{side} + S_{bottom})/2 \times S_{study}$

$= 0.4275$

$S = .4275 \times 1.32$ stars/proton

$S = .564$ stars/proton

Scaling to activity from reference 1, assuming 3.5×10^{17} protons/year[3]

$$A_{H3} = 0.046 \text{ nCi/yr}$$

$$= 1.47 \text{ nCi}/\ell$$

This is to be compared with the current EPA guideline of 20 nCi/ℓ.

Under more reasonable assumptions and removing any "safety factors" in S_{study} the tritium level is even further below the guidelines.

---

1. A. M. Jonckheere, "Proposal for the Target and Dump Area of the High Intensity M1 Area", 27 Nov. 1979.

2. A. M. Jonckheere, "Aquifer Dilution Factors of Ground Water Produced Around Fermilab Targets and Dumps", TM-838, 1 Dec. 1978.

3. "Design Report, 1979, Superconducting Accelerator" Fermi National Accelerator Laboratory, May, 1979.

Appendix IVa

Fermilab

T. E. Toohig
Sept. 7, 1979

TM-929

NOTE ON THE DESIGN OF THE EXTERNAL ABORT DUMP AT C0

The design of an external abort dump for the Main Ring and the Energy Doubler must take into account the instantaneous and long-term heating of the dump by the beam, possible radioactive contamination of the ground water, and possible dynamic radiation problems. A design incorporating these considerations is shown in Figure 1.

The question of possible radioactive contamination of the ground water is treated in a separate note where it is shown that the levels of radiation to be expected from the Doubler are up to four orders of magnitude lower than the EPA guidelines.

The problem of instantaneous heating of the dump by the one-turn extraction of the full intensity beam is addressed by using BeO slabs for the primary cores of the dump. This is modeled on the Neutrino production target.* The aluminum volume surrounding the cores provides a heat sink for longer term heating. This is supplemented by cooling loops attached to the exterior of the aluminum.

The remaining problem to be addressed is that of dynamic radiation. The beams are aborted at the level

---

*TM-825, J. Grimson, Target for Neutrino Beams, October 12, 1978.
CERN LAB II/BT/74-1, W. Kalbreier, W.C. Middlekoop, P. Sievers, External Targets at the SPS
CERN LAB II/BT/74-4, K. Teutenberg, P. Sievers, W.C. Middlekoop, Absorber Blocks for Internal and External Beam Dumping at the SPS

of the accelerators, i.e. 723', 4.5" for the Doubler and 725', 6" for the Main Ring. The surface elevation above the dump is 738' while the top of the dump is at 730', leaving 8' of overburden. This is equivalent to 20' of soil over the Main Ring dump and an additional 3' over the Doubler dump.

In the forward direction the surface contours drop to 731' rising to 747' at Butterfield Road. The distance to the site boundary at Butterfield Road is 1.7 km. The range for 1000 GeV muons is 1.7 to 2 km, depending on which energy loss mechanisms are invoked.* To minimize any problems of off-site muon leakage 5' long downstream cores of depleted uranium have been incorporated into the dump. The uranium is sealed in evacuated containers.

The muon energy loss per gm/cm^2 varies dramatically as a function of the Z of the absorber at Tevatron energies.* Folding in the difference in density of uranium and iron the uranium is at least 4½ times as effective in stopping muons and somewhat more effective if you turn on bremsstrahlung and nuclear interactions. In addition, the surviving muons are diluted by a factor of 6 by the difference in multiple scattering between iron and uranium.

$\rho_{Fe} = 7.8 - 7.9\ gm/cm^3$, $\rho_U = 18.7$ $\Big\}$ $R = 2.40 - 2.37$

$\frac{(dE/dx)_{U,1TeV}}{(dE/dx)_{Fe,1TeV}} = 1.89$ for Coul. & pair prod.

$= \infty$ for Coul., pair prod., bremsst., nuclear

*TM-286, Muon dE/dx and Range Tables for Tevatron Energies, G. Koizumi, May 9, 1978.

Appendix IVb

TM-929

Fermilab

September 25, 1979

MEMO TO: File

FROM: T. E. Toohig TET

SUBJECT: POSITIONING OF A URANIUM CORE IN THE DOUBLER ABORT DUMP

At Tevatron energies it is advantageous to utilize a uranium core in the abort dump to absorb and scatter muons. This is detailed in a note of September 7. A question has been raised about plutonium production in such a configuration. This problem may be obviated by a consideration of the excellent calorimeter data of J. Steinberger.[1] By extrapolation of Steinberger's data the length corresponding to 95% of the containment of the shower at 1 TeV is 780 gm/cm^2, which in the dump as designed is 27 inches upstream of the uranium core. The cascade falls off with an effective length of λ = 220 gm/cm^2 so that only 0.5% of the cascade energy passes into the uranium. This is probably all muons so there should be no problem with plutonium production.

Steinberger has also measured the "shower length", defined as the length where the average particle number goes below one. The shower length at 1 TeV is 1833 gm/cm^2 corresponding to 62 inches of iron behind the Be core. If one wanted to be extremely cautious and adopt the "shower length" as the acceptable criterion for hadron containment before entering uranium, it would suffice to shift the uranium core an additional two feet back in the dump as shown in the marked up sketch attached.

[1] Steinberger et al, Nuclear Inst. and Methods, 151 (1978), 69-80.

TET:eg

Attach.

cc:
J. R. Orr
H. Edwards
H. Jostlein
L. Coulson
H. Casebolt
D. Cossairt
F. Turkot

NATIONAL ACCELERATOR LABORATORY

ENGINEERING NOTE

SECTION	PROJECT	SERIAL-CATEGORY	PAGE
ED	Abort		6

SUBJECT: Abort assembly

NAME: T E Toohig

DATE: 8-22-79

REVISION DATE:

TM-929

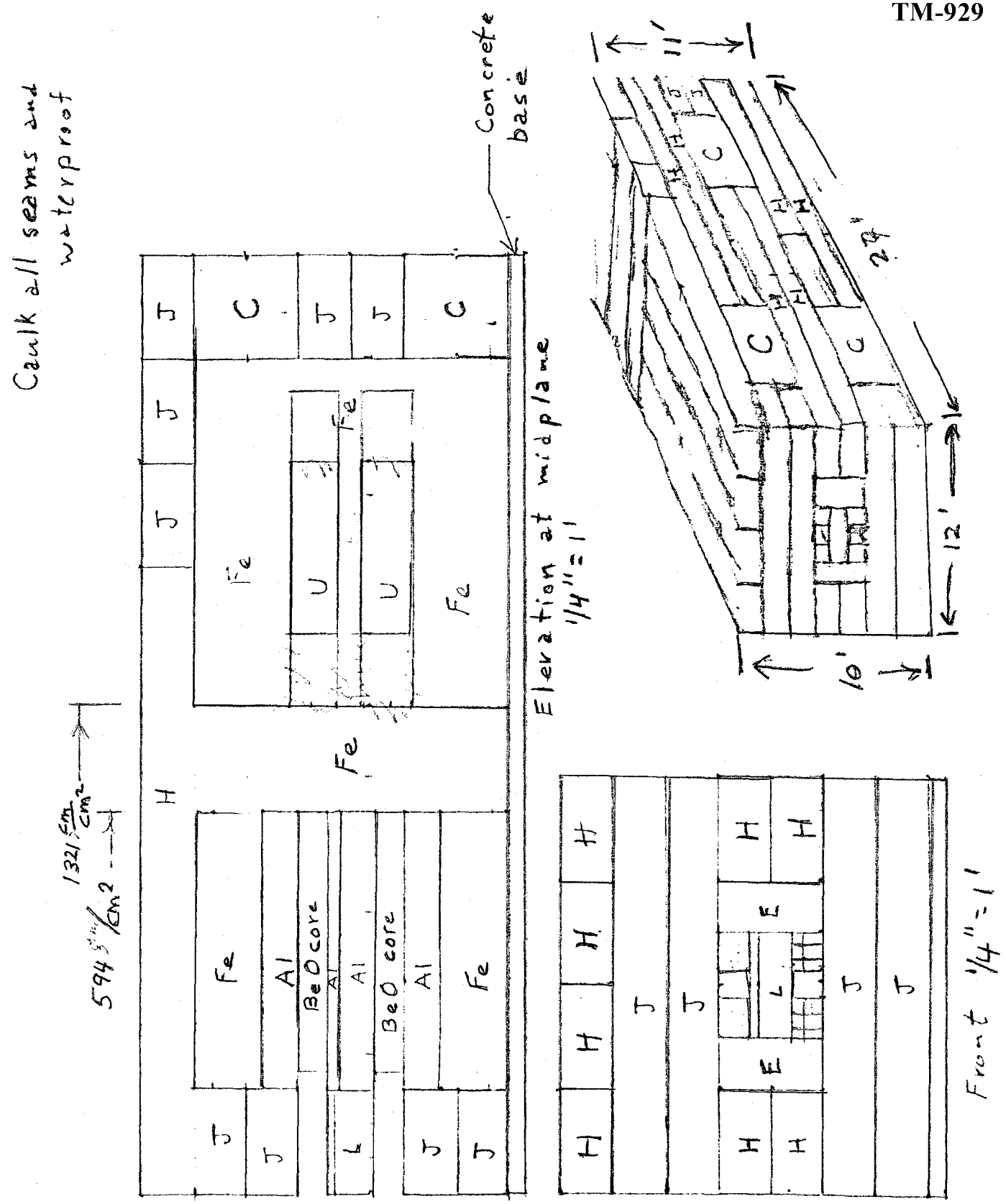

Appendix IVa

TM-929

Fermilab

November 1, 1979

MEMO TO: F. Turkot

FROM: T. E. Toohig TET

SUBJECT: THE QUESTION OF PLUTONIUM PRODUCTION IN THE URANIUM OF THE TEVATRON ABORT DUMP

I have examined the question of plutonium production in the depleted U^{238} muon absorber for the abort dump using the data of Steinberger, et al. Steinberger, et al have provided extensive data on hadron showers from 15-140 GeV, a factor of 10. The various quantities fall nicely on straight lines on semi-log paper so extrapolation of another factor of ten to 1 TeV should be quite straightforward. See the attached plot, as an example.

The absorber in the abort dump design is given in Table I.

TABLE I

Absorber Parameters

Material	ρ (gm/cm^3)	λ_{abs} (cm)	λ_{abs} (gm/cm^2)	Length (gm/cm^2)	Length (cm)	Length (L/λ_{abs})
BeO	2.846	26	74	650.6	228.6	8.792
Fe	7.87	17.1*	135	713.2	91.4	5.283
U	18.95	12	227.4	3898.0	205.7	17.142
Concrete	2.40	44.6	107	219.4	91.4	2.049

*Ranft, Part. Acc. 3, 149 $\lambda_{abs,\rho}$(Fe) = 123 gm/cm2.

*Steinberger, NIM 15 λ_{abs,π^-}(Fe) = 19 cm (no ρ given)

= 149 gm/cm^2 for ρ = 7.87

Steinberger finds that the absorption length in iron, λ_{abs}, is 19 cm. By shifting the U by 26 inches downstream I make the total length of absorber upstream of the uranium equal to the 1 TeV shower length. The shower length is defined to be the length required to

reduce the transversely integrated flux to one equivalent minimum-ionizing particle. Since some muons are produced in the shower, it is safe to assume that this is a muon. (This is also consistent with the experience behind, e.g. the E439 beam dump.)

What does remain to be considered, however, when dealing with statistics of 3.5×10^{17} protons/year aborted is the attenuated proton beam reaching the uranium. The length to the uranium is 17.56 λ_{abs} for an attenuation of 2.37×10^{-8}. Therefore

$$\boxed{I_{incident} = 2.64 \times 10^{2} \text{ protons/sec}} \quad \text{for } 3.5 \times 10^{17} \text{ p/yr aborted}$$

Now go to Willis, et al with their uranium calorimeter data.

From Steinberger, the buildup is linear with energy - α 10 for x 10 E_o.

Willis finds 20 neutrons/GeV by spallation of U^{238} and
29.5 neutrons/GeV from fission
total 49.5 neutrons/GeV - not far from Van Ginneken's 60 n/GeV.

If we assume with Van Ginneken that all the neutrons finally wind up in:

$$U^{238}(n,\alpha)U^{239} \rightarrow np^{239} \rightarrow Pu^{239}$$

then each 1 TeV proton incident produces 50K Pu^{239}.
It requires $\frac{No}{50K} = 4.8 \times 10^{16}$ protons to produce 1 gram of Pu^{239} or:
$T = 1.9 \times 10^{14}$ seconds

$$\boxed{T = 6 \times 10^{6} \text{ years/gm}}$$

Further, since it is produced within the U^{238} block, one ton of U^{238} must be leached away to get at the 1/6 of a microgram of Pu^{239} produced in one year.

This concentration is an order of magnitude less than what is found in concentrated, naturally occurring pitchblende ores.

TET:eg

cc: J. R. Orr, H. Edwards. H. Jostlein, H. Casebolt, A. L. Read, K. Cahill

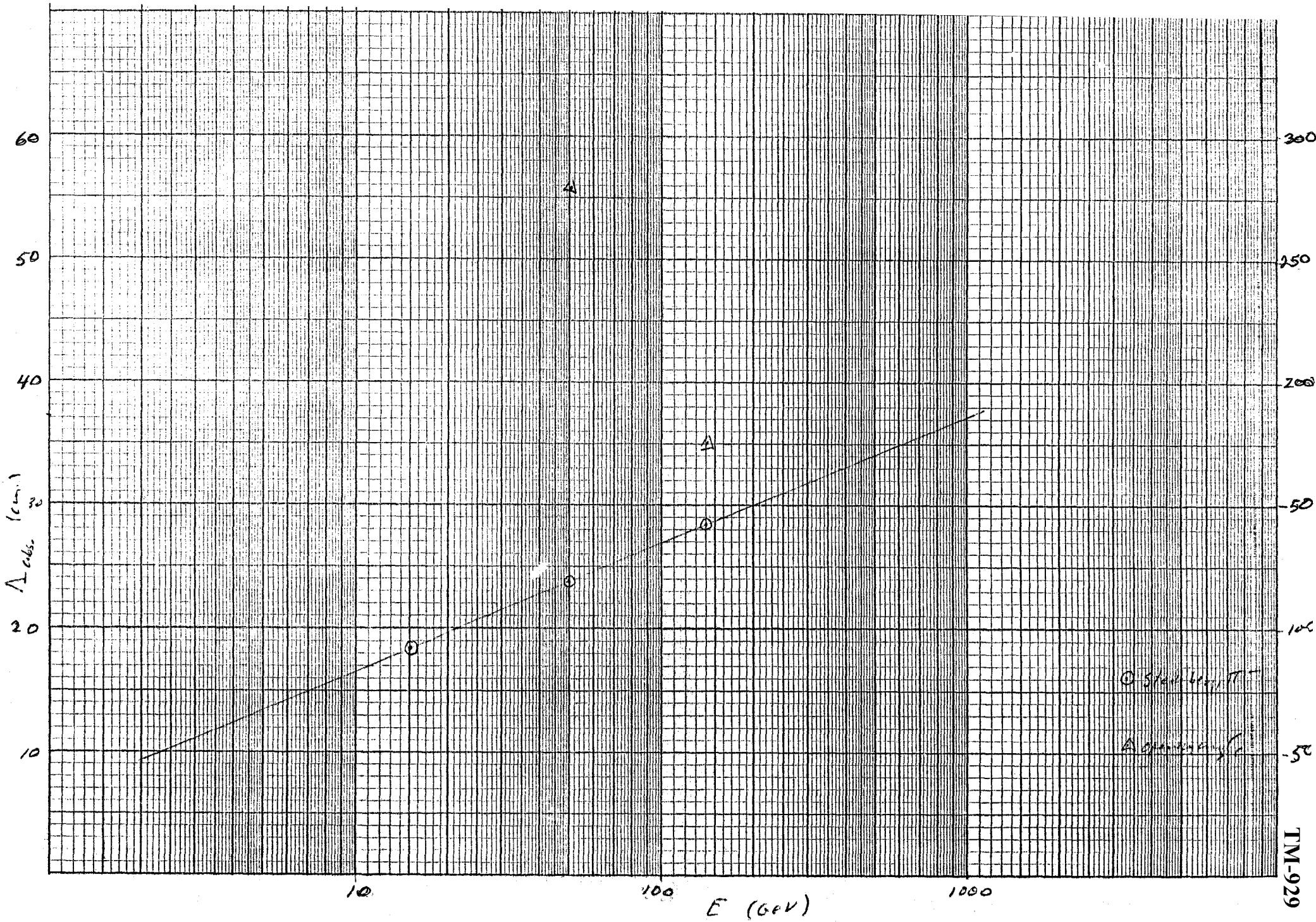

TM-929

STAR DENSITY IN UNITS OF STARS/(CM3*INC.PARTICLE) AS A FUNCTION OF DEPTH(DOWN) AND RADIUS(ACROSS) IN CM
FOR PARTICLES OF KIND 4
(1=PROTONS,2=NEUTRONS,3=PIONS,4=ALL STARS,5=ENERGY DENSITY IN GEV/(CM3*INC.PARTICLE),6=RELATIVE ERROR OF ALL STAR DENSITY

Fe | cct

		75.000 77.500	77.500 80.000	80.000 82.500	82.500 85.000	85.000 87.500	87.500 90.000	90.000 92.500	92.500 95.000	95.000 97.500	97.500 100.000
-0.00	7.28	0.42E-06	0.21E-06	0.22E-06	0.74E-07	0.73E-07	0.61E-07	0.54E-07	0.67E-07	0.53E-07	0.41E-07
7.28	14.56	0.38E-06	0.36E-06	0.27E-06	0.92E-07	0.92E-07	0.78E-07	0.59E-07	0.66E-07	0.61E-07	0.66E-07
14.56	21.84	0.59E-06	0.40E-06	0.28E-06	0.17E-06	0.12E-06	0.94E-07	0.94E-07	0.96E-07	0.81E-07	0.73E-07
21.84	29.12	0.54E-06	0.46E-06	0.47E-06	0.16E-06	0.11E-06	0.13E-06	0.13E-06	0.10E-06	0.86E-07	0.94E-07
29.12	36.40	0.97E-06	0.80E-06	0.61E-06	0.21E-06	0.18E-06	0.16E-06	0.15E-06	0.15E-06	0.14E-06	0.12E-06
36.40	43.68	0.97E-06	0.83E-06	0.62E-06	0.27E-06	0.22E-06	0.18E-06	0.18E-06	0.21E-06	0.16E-06	0.13E-06
43.68	50.96	0.16E-05	0.98E-06	0.93E-06	0.35E-06	0.30E-06	0.22E-06	0.21E-06	0.24E-06	0.18E-06	0.20E-06
50.96	58.24	0.21E-05	0.18E-05	0.13E-05	0.43E-06	0.40E-06	0.32E-06	0.35E-06	0.37E-06	0.28E-06	0.24E-06
58.24	65.52	0.21E-05	0.18E-05	0.16E-05	0.60E-06	0.55E-06	0.36E-06	0.43E-06	0.44E-06	0.31E-06	0.27E-06
65.52	72.80	0.29E-05	0.21E-05	0.17E-05	0.67E-06	0.54E-06	0.43E-06	0.41E-06	0.48E-06	0.39E-06	0.56E-06
72.80	80.08	0.32E-05	0.28E-05	0.20E-05	0.79E-06	0.73E-06	0.64E-06	0.58E-06	0.68E-06	0.75E-06	0.43E-06
80.08	87.36	0.42E-05	0.34E-05	0.26E-05	0.11E-05	0.78E-06	0.72E-06	0.89E-06	0.11E-05	0.11E-05	0.60E-06
87.36	94.64	0.42E-05	0.39E-05	0.31E-05	0.17E-05	0.12E-05	0.16E-05	0.19E-05	0.11E-05	0.97E-06	0.94E-06
94.64	101.92	0.75E-05	0.70E-05	0.68E-05	0.34E-05	0.33E-05	0.23E-05	0.23E-05	0.29E-05	0.24E-05	0.24E-05
101.92	109.20	0.26E-04	0.26E-04	0.31E-04	0.13E-04	0.13E-04	0.87E-05	0.52E-05	0.41E-05	0.64E-05	0.36E-05
109.20	116.48	0.17E-04	0.15E-04	0.10E-04	0.50E-05	0.56E-05	0.42E-05	0.29E-05	0.37E-05	0.26E-05	0.30E-05
116.48	123.76	0.12E-04	0.95E-05	0.10E-04	0.32E-05	0.27E-05	0.25E-05	0.32E-05	0.18E-05	0.20E-05	0.16E-05
123.76	131.04	0.84E-05	0.10E-04	0.82E-05	0.30E-05	0.23E-05	0.25E-05	0.20E-05	0.18E-05	0.21E-05	0.20E-05
131.04	138.32	0.86E-05	0.78E-05	0.64E-05	0.22E-05	0.20E-05	0.18E-05	0.17E-05	0.19E-05	0.16E-05	0.14E-05
138.32	145.60	0.80E-05	0.71E-05	0.56E-05	0.23E-05	0.19E-05	0.15E-05	0.14E-05	0.16E-05	0.13E-05	0.13E-05
145.60	152.88	0.92E-05	0.72E-05	0.42E-05	0.22E-05	0.19E-05	0.18E-05	0.17E-05	0.16E-05	0.13E-05	0.12E-05
152.88	160.16	0.15E-04	0.99E-05	0.69E-05	0.27E-05	0.24E-05	0.17E-05	0.16E-05	0.19E-05	0.15E-05	0.12E-05
160.16	167.44	0.15E-04	0.16E-04	0.96E-05	0.35E-05	0.30E-05	0.24E-05	0.21E-05	0.19E-05	0.16E-05	0.13E-05
167.44	174.72	0.12E-04	0.11E-04	0.11E-04	0.42E-05	0.29E-05	0.24E-05	0.29E-05	0.23E-05	0.21E-05	0.16E-05
174.72	182.00	0.13E-04	0.11E-04	0.90E-05	0.30E-05	0.28E-05	0.25E-05	0.20E-05	0.18E-05	0.19E-05	0.20E-05
182.00	189.28	0.12E-04	0.97E-05	0.77E-05	0.27E-05	0.25E-05	0.21E-05	0.17E-05	0.19E-05	0.18E-05	0.17E-05
189.28	196.56	0.16E-04	0.13E-04	0.88E-05	0.30E-05	0.30E-05	0.25E-05	0.20E-05	0.24E-05	0.19E-05	0.15E-05
196.56	203.84	0.28E-04	0.20E-04	0.14E-04	0.54E-05	0.41E-05	0.31E-05	0.30E-05	0.32E-05	0.22E-05	0.21E-05
203.84	211.12	0.25E-04	0.25E-04	0.20E-04	0.70E-05	0.45E-05	0.37E-05	0.42E-05	0.37E-05	0.27E-05	0.25E-05
211.12	218.40	0.20E-04	0.19E-04	0.15E-04	0.64E-05	0.47E-05	0.35E-05	0.42E-05	0.47E-05	0.29E-05	0.25E-05
218.40	225.68	0.20E-04	0.17E-04	0.13E-04	0.49E-05	0.38E-05	0.38E-05	0.28E-05	0.40E-05	0.28E-05	0.29E-05
225.68	232.96	0.13E-04	0.12E-04	0.10E-04	0.38E-05	0.32E-05	0.33E-05	0.29E-05	0.26E-05	0.25E-05	0.26E-05
232.96	240.24	0.14E-04	0.12E-04	0.81E-05	0.35E-05	0.39E-05	0.30E-05	0.22E-05	0.21E-05	0.20E-05	0.21E-05
240.24	247.52	0.12E-04	0.96E-05	0.83E-05	0.31E-05	0.24E-05	0.20E-05	0.22E-05	0.19E-05	0.20E-05	0.15E-05
247.52	254.80	0.12E-04	0.87E-05	0.74E-05	0.30E-05	0.25E-05	0.19E-05	0.18E-05	0.19E-05	0.16E-05	0.19E-05
254.80	262.08	0.95E-05	0.90E-05	0.59E-05	0.24E-05	0.22E-05	0.19E-05	0.20E-05	0.18E-05	0.22E-05	0.15E-05
262.08	269.36	0.98E-05	0.73E-05	0.64E-05	0.25E-05	0.37E-05	0.22E-05	0.32E-05	0.21E-05	0.20E-05	0.14E-05
269.36	276.64	0.14E-04	0.17E-04	0.16E-04	0.50E-05	0.22E-05	0.24E-05	0.37E-05	0.21E-05	0.16E-05	0.19E-05
276.64	283.92	0.98E-05	0.10E-04	0.83E-05	0.74E-05	0.50E-05	0.35E-05	0.35E-05	0.25E-05	0.18E-05	0.23E-05
283.92	291.20	0.12E-04	0.15E-04	0.79E-05	0.37E-05	0.27E-05	0.36E-05	0.27E-05	0.27E-05	0.22E-05	0.27E-05
291.20	298.48	0.90E-05	0.20E-04	0.23E-04	0.41E-05	0.32E-05	0.23E-05	0.23E-05	0.27E-05	0.18E-05	0.19E-05
298.48	305.76	0.82E-05	0.92E-05	0.75E-05	0.26E-05	0.36E-05	0.35E-05	0.20E-05	0.17E-05	0.17E-05	0.23E-05
305.76	313.04	0.90E-05	0.69E-05	0.57E-05	0.21E-05	0.20E-05	0.19E-05	0.23E-05	0.18E-05	0.19E-05	0.11E-05
313.04	320.32	0.86E-05	0.50E-05	0.50E-05	0.21E-05	0.22E-05	0.16E-05	0.17E-05	0.18E-05	0.19E-05	0.12E-05
320.32	327.60	0.61E-05	0.32E-05	0.32E-05	0.25E-05	0.26E-05	0.24E-05	0.17E-05	0.19E-05	0.22E-05	0.16E-05
327.60	334.88	0.59E-05	0.46E-05	0.42E-05	0.44E-05	0.31E-05	0.23E-05	0.23E-05	0.21E-05	0.20E-05	0.18E-05
334.88	342.16	0.62E-05	0.49E-05	0.42E-05	0.37E-05	0.36E-05	0.31E-05	0.28E-05	0.20E-05	0.26E-05	0.20E-05
342.16	349.44	0.68E-05	0.47E-05	0.55E-05	0.37E-05	0.35E-05	0.35E-05	0.34E-05	0.27E-05	0.21E-05	0.31E-05
349.44	356.72	0.62E-05	0.59E-05	0.40E-05	0.51E-05	0.39E-05	0.32E-05	0.28E-05	0.25E-05	0.28E-05	0.21E-05
356.72	364.00	0.58E-05	0.73E-05	0.55E-05	0.55E-05	0.50E-05	0.43E-05	0.40E-05	0.33E-05	0.28E-05	0.27E-05

STAR DENSITY IN UNITS OF STARS/(CM3*INC.PARTICLE) AS A FUNCTION OF DEPTH(DOWN) AND RADIUS(ACROSS) IN CM
FOR PARTICLES OF KIND 4
(1=PROTONS,2=NEUTRONS,3=PIONS,4=ALL STARS,5=ENERGY DENSITY IN GEV/(CM3*INC.PARTICLE),6=RELATIVE ERROR OF ALL STAR DENSITY)

		100.000 102.500	102.500 105.000	105.000 107.500	107.500 110.000	110.000 112.500	112.500 115.000	115.000 117.500	117.500 120.000	120.000 122.500	122.500 125.000
-0.00	7.28	0.51E-07	0.47E-07	0.43E-07	0.77E-07	0.96E-07	0.69E-07	0.98E-07	0.78E-07	0.71E-07	0.33E-07
7.28	14.56	0.51E-07	0.47E-07	0.41E-07	0.11E-06	0.83E-07	0.28E-06	0.13E-06	0.55E-07	0.50E-07	0.17E-06
14.56	21.84	0.68E-07	0.80E-07	0.67E-07	0.12E-06	0.49E-06	0.11E-05	0.39E-06	0.78E-06	0.49E-06	0.18E-06
21.84	29.12	0.95E-07	0.90E-07	0.72E-07	0.15E-06	0.49E-06	0.77E-06	0.77E-06	0.44E-06	0.14E-06	0.20E-06
29.12	36.40	0.11E-06	0.11E-06	0.96E-07	0.20E-06	0.21E-06	0.18E-06	0.14E-06	0.11E-06	0.21E-06	0.21E-06
36.40	43.68	0.13E-06	0.13E-06	0.13E-06	0.23E-06	0.21E-06	0.23E-06	0.25E-06	0.16E-06	0.12E-06	0.11E-06
43.68	50.96	0.15E-06	0.18E-06	0.14E-06	0.36E-06	0.40E-06	0.33E-06	0.23E-06	0.15E-06	0.13E-06	0.12E-06
50.96	58.24	0.24E-06	0.23E-06	0.27E-06	0.52E-06	0.46E-06	0.29E-06	0.29E-06	0.26E-06	0.20E-06	0.16E-06
58.24	65.52	0.33E-06	0.42E-06	0.27E-06	0.45E-06	0.68E-06	0.52E-06	0.39E-06	0.25E-06	0.22E-06	0.20E-06
65.52	72.80	0.50E-06	0.34E-06	0.36E-06	0.74E-06	0.64E-06	0.56E-06	0.40E-06	0.35E-06	0.36E-06	0.24E-06
72.80	80.08	0.61E-06	0.43E-06	0.34E-06	0.85E-06	0.90E-06	0.78E-06	0.59E-06	0.45E-06	0.42E-06	0.36E-06
80.08	87.36	0.80E-06	0.80E-06	0.49E-06	0.13E-05	0.12E-05	0.11E-05	0.67E-06	0.56E-06	0.54E-06	0.61E-06
87.36	94.64	0.10E-05	0.93E-06	0.89E-06	0.15E-05	0.17E-05	0.16E-05	0.18E-05	0.97E-06	0.12E-05	0.12E-05
94.64	101.92	0.20E-05	0.30E-05	0.25E-05	0.27E-05	0.34E-05	0.24E-05	0.24E-05	0.11E-05	0.15E-05	0.98E-06
101.92	109.20	0.23E-05	0.29E-05	0.27E-05	0.44E-05	0.33E-05	0.36E-05	0.45E-05	0.12E-05	0.10E-05	0.13E-05
109.20	116.48	0.19E-05	0.19E-05	0.17E-05	0.40E-05	0.40E-05	0.33E-05	0.28E-05	0.38E-05	0.21E-05	0.26E-05
116.48	123.76	0.18E-05	0.18E-05	0.14E-05	0.27E-05	0.22E-05	0.24E-05	0.21E-05	0.13E-05	0.98E-06	0.13E-05
123.76	131.04	0.13E-05	0.15E-05	0.14E-05	0.27E-05	0.23E-05	0.24E-05	0.14E-05	0.14E-05	0.93E-06	0.10E-05
131.04	138.32	0.11E-05	0.14E-05	0.11E-05	0.18E-05	0.20E-05	0.20E-05	0.16E-05	0.81E-06	0.11E-05	0.95E-06
138.32	145.60	0.14E-05	0.11E-05	0.11E-05	0.20E-05	0.18E-05	0.20E-05	0.11E-05	0.10E-05	0.96E-06	0.98E-06
145.60	152.88	0.13E-05	0.11E-05	0.12E-05	0.21E-05	0.18E-05	0.19E-05	0.14E-05	0.97E-06	0.91E-06	0.83E-06
152.88	160.16	0.12E-05	0.11E-05	0.11E-05	0.22E-05	0.19E-05	0.17E-05	0.14E-05	0.11E-05	0.97E-06	0.73E-06
160.16	167.44	0.13E-05	0.12E-05	0.10E-05	0.19E-05	0.19E-05	0.18E-05	0.15E-05	0.94E-06	0.96E-06	0.78E-06
167.44	174.72	0.17E-05	0.12E-05	0.11E-05	0.23E-05	0.18E-05	0.20E-05	0.14E-05	0.96E-06	0.93E-06	0.93E-06
174.72	182.00	0.14E-05	0.14E-05	0.14E-05	0.26E-05	0.24E-05	0.23E-05	0.15E-05	0.14E-05	0.11E-05	0.11E-05
182.00	189.28	0.13E-05	0.16E-05	0.13E-05	0.30E-05	0.20E-05	0.22E-05	0.20E-05	0.13E-05	0.12E-05	0.11E-05
189.28	196.56	0.18E-05	0.14E-05	0.14E-05	0.28E-05	0.26E-05	0.25E-05	0.21E-05	0.15E-05	0.13E-05	0.12E-05
196.56	203.84	0.13E-05	0.21E-05	0.17E-05	0.40E-05	0.35E-05	0.29E-05	0.22E-05	0.14E-05	0.15E-05	0.13E-05
203.84	211.12	0.24E-05	0.21E-05	0.18E-05	0.39E-05	0.32E-05	0.31E-05	0.22E-05	0.18E-05	0.17E-05	0.14E-05
211.12	218.40	0.22E-05	0.24E-05	0.18E-05	0.36E-05	0.92E-05	0.53E-05	0.43E-05	0.32E-05	0.29E-05	0.28E-05
218.40	225.68	0.31E-05	0.27E-05	0.19E-05	0.50E-05	0.71E-05	0.89E-05	0.72E-05	0.57E-05	0.39E-05	0.28E-05
225.68	232.96	0.22E-05	0.29E-05	0.22E-05	0.43E-05	0.36E-05	0.39E-05	0.32E-05	0.22E-05	0.24E-05	0.23E-05
232.96	240.24	0.20E-05	0.18E-05	0.16E-05	0.47E-05	0.29E-05	0.33E-05	0.73E-05	0.23E-05	0.19E-05	0.21E-05
240.24	247.52	0.16E-05	0.17E-05	0.13E-05	0.24E-05	0.27E-05	0.33E-05	0.58E-05	0.62E-05	0.22E-05	0.59E-05
247.52	254.80	0.13E-05	0.14E-05	0.14E-05	0.22E-05	0.22E-05	0.23E-05	0.22E-05	0.22E-05	0.25E-05	0.35E-05
254.80	262.08	0.13E-05	0.13E-05	0.14E-05	0.24E-05	0.22E-05	0.25E-05	0.18E-05	0.14E-05	0.13E-05	0.10E-05
262.08	269.36	0.15E-05	0.12E-05	0.14E-05	0.22E-05	0.25E-05	0.23E-05	0.17E-05	0.12E-05	0.11E-05	0.14E-05
269.36	276.64	0.15E-05	0.13E-05	0.15E-05	0.30E-05	0.19E-05	0.18E-05	0.16E-05	0.12E-05	0.99E-06	0.86E-06
276.64	283.92	0.17E-05	0.13E-05	0.10E-05	0.20E-05	0.24E-05	0.20E-05	0.11E-05	0.13E-05	0.98E-06	0.74E-06
283.92	291.20	0.15E-05	0.13E-05	0.20E-05	0.24E-05	0.24E-05	0.25E-05	0.22E-05	0.13E-05	0.11E-05	0.76E-06
291.20	298.48	0.18E-05	0.15E-05	0.17E-05	0.26E-05	0.18E-05	0.28E-05	0.18E-05	0.12E-05	0.12E-05	0.11E-05
298.48	305.76	0.12E-05	0.13E-05	0.15E-05	0.26E-05	0.23E-05	0.23E-05	0.17E-05	0.18E-05	0.54E-05	0.22E-05
305.76	313.04	0.11E-05	0.14E-05	0.13E-05	0.15E-05	0.22E-05	0.24E-05	0.14E-05	0.99E-06	0.21E-05	0.27E-05
313.04	320.32	0.17E-05	0.11E-05	0.11E-05	0.22E-05	0.23E-05	0.18E-05	0.15E-05	0.92E-06	0.12E-05	0.13E-05
320.32	327.60	0.21E-05	0.17E-05	0.14E-05	0.93E-06	0.96E-06	0.97E-06	0.80E-06	0.68E-06	0.57E-06	0.61E-06
327.60	334.88	0.14E-05	0.22E-05	0.18E-05	0.13E-05	0.12E-05	0.11E-05	0.92E-06	0.70E-06	0.63E-06	0.65E-06
334.88	342.16	0.14E-05	0.12E-05	0.12E-05	0.11E-05	0.11E-05	0.17E-05	0.13E-05	0.10E-05	0.96E-06	0.72E-06
342.16	349.44	0.19E-05	0.21E-05	0.18E-05	0.16E-05	0.12E-05	0.12E-05	0.12E-05	0.12E-05	0.83E-06	0.76E-06
349.44	356.72	0.19E-05	0.16E-05	0.17E-05	0.13E-05	0.11E-05	0.11E-05	0.11E-05	0.11E-05	0.79E-06	0.66E-06
356.72	364.00	0.19E-05	0.21E-05	0.15E-05	0.15E-05	0.15E-05	0.15E-05	0.83E-06	0.10E-05	0.12E-05	0.90E-06

$5\times10^{-6} * 9\times10^{-6} = 5\times10^{-12}\ \frac{rad/h}{p/sec}$